COMPUTATIONAL FLUID DYNAMICS ANALYSIS OF NO_x REDUCTION BY AMMONIA INJECTION IN THE MAN B&W 7S50MC MARINE ENGINE

(DOI No: 10.3940/rina.ijme.2014.a3.286)

M I Lamas, C G Rodríguez and **J D Rodríguez,** University of Coruña, Spain, **J Telmo,** University of Santiago de Compostela, Spain

SUMMARY

Taking into account the importance of NO_x (nitrogen oxides) emissions from marine engines and the current increasingly restrictive legislation, this work aims to develop a numerical model to study NO_x reduction. To this end, direct injection of NH_3 (ammonia) into the combustion chamber was proposed in the MAN B&W 7S50MC marine engine. The numerical model was employed to analyze several injection temperatures, injection timings and ammonia to fuel ratios, obtaining NO_x reductions of almost 60%. Besides, a comparison between ammonia injection and water injection was done. The results showed that ammonia is more efficient than water to reduce NO_x with a negligible influence on other pollutants such as CO (carbon monoxide) and HC (hydrocarbons). Nevertheless, ammonia is efficient in a very restrictive temperature and injection timing range. This numerical model was compared with experimental measurements, obtaining satisfactory results which validate the work.

NOMENCLATURE

C	Concentration (kmol m^3)
f	Mass fraction (-)
H	Enthalpy (J kg^{-1})
k	Rate constant (m^3 $kmol^{-1}$ s^{-1})
m	Number of reactions (-)
MW	Molecular weight (kg $kmol^{-1}$)
N	Number of species (-)
p	Pressure (Pa)
S	Energy source term (J s^{-1} m^{-3})
t	Time (s)
T	Temperature (K)
u	Velocity (m s^{-1})

Greek symbols

ϕ	Diameter (mm)
μ	Dynamic viscosity (Pa s)
μ_t	Turbulent viscosity (Pa s)
ρ	Density (kg m^{-3})
σ	Prandtl number (-)
σ_h	Turbulent Prandtl number (-)
σ_ζ	Turbulent Schmidt number (-)
τ_{ij}	Stress tensor (Pa)
v	Stoichiometric coefficient (-)
ω	Net rate of production of a specie by chemical reaction (kg m^{-3} s)

1. INTRODUCTION

Nowadays, diesel engines power most of the ships in the world. Despite its efficiency, marine engines emit important quantities of NO_x, SO_x and particulates. Merchant ships in international traffic are subjected to the International Maritime Organization (IMO). Particularly, the IMO Marpol Annex VI limits SO_x from marine fuels and NO_x emissions from marine engines. Apart from these international limitations, some regions have developed regional and national tougher limits. Due to these increasingly restrictive regulations, many methods have been developed over the last few years to reduce diesel NO_x emissions. Some of these methods, called primary measures, consist on reducing the amount of NO_x during combustion. Concerning marine engines, several primary measures have been studied in the literature such as modification of injection parameters [1-9], water addition [10, 11], EGR [11-14], etc. On the other hand, other NO_x reduction methods, called secondary measures, remove NO_x from the exhaust gases by post-combustion cleaning techniques. The most employed secondary measures in diesel engines are SNCR (selective non-catalytic reduction) and SCR (selective catalytic reduction). The former consists on reducing NO_x to nitrogen (N_2) using a nitrogen reducing agent such as ammonia, urea ($CO[NH_2]_2$), cyanuric acid ($[HNCO]_3$), hydrocarbons, etc. SNCR process has been successfully implemented in stationary power plants boilers and industrial furnaces. The main disadvantage of SNCR is that this is only efficient in a narrow temperature window centered at approximately 1200K (±100), Lamas and Rodriguez [15]. Flue gas from marine engines does not reach this temperature, and re-heating them is complicated. For this reason, catalysts are commonly employed to reduce NO_x from exhaust gas, what is called SCR. The main disadvantages of SCR are the poor durability and price. Besides, an additional space is required for the catalytic reactor. Several works about SCR in marine engines can be found in the literature [16, 17].

Taking into account the disadvantages of SCR and the temperature requirements of SNCR, the present work studied the possibility of injecting the reducing agent directly into the combustion chamber [18-20]. The marine engine MAN B&W 7S50MC was analyzed numerically using ammonia as NO_x reducing agent. The remainder of this paper is structured as follows. Section 2 describes the computation of NO_x reduction by ammonia injection. Section 3 describes the engine analyzed and the

details of the numerical model and Section 4 indicates the results. Finally, the conclusions of this work are presented.

2. COMPUTATION OF NO_x REDUCTION BY AMMONIA INJECTION

This section describes the procedure employed to model numerically NO_x reduction by ammonia injection. First of all, the chemical kinetics models are described. After that, the implementation of the chemical models into a CFD code and finally a validation of the numerical model using experimental results obtained from the literature.

2.1 CHEMICAL KINETICS MODEL

Among all NO_x components, almost 100% is NO. SNCR of NO using ammonia was first described by Lyon in 1975 [21]. Since then, the kinetics of the process was intensively studied. The first kinetic model was proposed by Miller and Bowman [22], based on 73 reactions and 19 species. Other models are those of Glarborg *et al.* [23], involving 104 reactions and 22 species; Miler and Glarborg [24], involving 134 reactions and 24 species; etc. Simplified models are also available in the literature, for instance those of Brouwer *et al.* [25] and Duo *et al.* [26], based on two-reactions. As the simulation of a complex chemical model demands extremely high computational resources, the present work employed the simplified models of Brouwer *et al.* [25] and Duo *et al.* [26]. The reactions and rate constants of these are given in Tables 1 and 2 respectively.

Table 1. Reactions and rate constants of the model of Brouwer *et al.* [25].

Reaction	Reaction rate constant
$NH_3 + NO \xrightarrow{k_1} N_2 + H_2O + H$	$k_1 = 4.24x10^8 T^{1.50} e(-83600/RT)$
$NH_3 + O_2 \xrightarrow{k_2} NO + H_2O + H$	$k_2 = 3.50x10^5 T^{2.65} e(-125300/RT)$

Table 2. Reactions and rate constants of the model of Duo *et al.* [26].

Reaction	Reaction rate constant
$NH_3 + NO + 1/4O_2 \xrightarrow{k_1} N_2 + 3/2H_2O$	$k_1 = 2.45x10^{20} e(-58413/RT)$
$NH_3 + 5/4O_2 \xrightarrow{k_2} NO + 3/2H_2O$	$k_2 = 2.21x10^{14} e(-75837/RT)$

2.2 CFD MODEL

Given a set of *m* reactions which involve *N* species, Eq. (1), the local mass fraction of each species, f_k, can be expressed by Eq. (2), Versteeg and Malalasekera [27].

$$\sum_{k=1}^{N} v'_{kj} M_k \longrightarrow \sum_{k=1}^{N} v''_{kj} M_k \qquad j = 1, 2, \ldots, m \tag{1}$$

$$\frac{\partial}{\partial t}(\rho f_k) + \frac{\partial}{\partial x_i}(\rho u_i f_k) = \frac{\partial}{\partial x_i}\left(\frac{\mu_t}{\sigma_\varsigma}\frac{\partial f_k}{\partial x_i}\right) + \omega_k \tag{2}$$

In the equations above, v'_{kj} are stoichiometric coefficients of reactant species M_k in the reaction *j*, v''_{kj} are stoichiometric coefficients of product species M_k in the reaction *j*, *N* is the total number of species involved, ρ is the density, μ_t is the turbulent viscosity, σ_ς is the turbulent Smidth number and ω_k is the net rate of production of the specie *k* by chemical reaction, given by the molecular weigh multiplied by the production rate of a specie, Eq. (3).

$$\omega_k = MW_k \frac{\mathrm{d}C_k}{\mathrm{d}t} \tag{3}$$

where *MW* is the molecular weight and *C* the concentration. The net progress rate of reaction *j* is given by the production of the species M_k minus the destruction of the species M_k:

$$\frac{\mathrm{d}C_M}{\mathrm{d}t} = (v''_{kj} - v'_{kj}) k_j \prod_{k=1}^{N} (C_{M_k})^{v'_{kj}} \tag{4}$$

In the case of the chemical kinetic model of Browner *et al.* [25] indicated in Table 1, 6 species are involved NH_3, NO, N_2, H_2O, H, O_2. Eqs. (1-2) applied for 5 of these species are indicated by Eqs. (5-9). Since the mass fraction of all the species must sum to unity, one of the mass fractions can be determined as one minus the sum of the remaining mass fractions, Eq. (10). To minimize the numerical error, the 6th specie must be the one with the overall largest mass fraction, in this case N_2. The procedure employed to model the chemical reactions proposed by Duo *et al.* [26] is similar and thus not repeated again.

$$\frac{\partial}{\partial t}(\rho f_{NH_3}) + \frac{\partial}{\partial x_i}(\rho u_i f_{NH_3}) = \frac{\partial}{\partial x_i}\left(\frac{\mu_t}{\sigma_\varsigma}\frac{\partial f_{NH_3}}{\partial x_i}\right) + M_{NH_3}(-k_1 C_{NH_3} C_{NO} - k_2 C_{NH_3} C_{O_2}) \tag{5}$$

$$\frac{\partial}{\partial t}(\rho f_{NO}) + \frac{\partial}{\partial x_i}(\rho u_i f_{NO}) = \frac{\partial}{\partial x_i}\left(\frac{\mu_t}{\sigma_\varsigma}\frac{\partial f_{NO}}{\partial x_i}\right) + M_{NO}(-k_1 C_{NH_3} C_{NO} + k_2 C_{NH_3} C_{O_2}) \tag{6}$$

$$\frac{\partial}{\partial t}(\rho f_{H_2O}) + \frac{\partial}{\partial x_i}(\rho u_i f_{H_2O}) = \frac{\partial}{\partial x_i}\left(\frac{\mu_t}{\sigma_\varsigma}\frac{\partial f_{H_2O}}{\partial x_i}\right) + M_{H_2O}(k_1 C_{NH_3} C_{NO} + k_2 C_{NH_3} C_{O_2}) \tag{7}$$

$$\frac{\partial}{\partial t}(\rho f_H) + \frac{\partial}{\partial x_i}(\rho u_i f_H) = \frac{\partial}{\partial x_i}\left(\frac{\mu_t}{\sigma_\xi}\frac{\partial f_H}{\partial x_i}\right) + M_H(k_1 C_{NH_3} C_{NO} + k_2 C_{NH_3} C_{O_2}) \quad (8)$$

$$\frac{\partial}{\partial t}(\rho f_{O_2}) + \frac{\partial}{\partial x_i}(\rho u_i f_{O_2}) = \frac{\partial}{\partial x_i}\left(\frac{\mu_t}{\sigma_\xi}\frac{\partial f_{O_2}}{\partial x_i}\right) + M_{O_2}(-k_2 C_{NH_3} C_{O_2}) \quad (9)$$

$$\sum_{k=1}^{N} f_k = 1 \quad (10)$$

In addition to Eqs. (5-10), a fluid dynamics problem also requires the field equations of conservation of mass, momentum and energy, Eqs. (11-13) respectively.

$$\frac{\partial \rho}{\partial t} + \frac{\partial}{\partial x_i}(\rho u_i) = 0 \quad (11)$$

$$\frac{\partial}{\partial t}(\rho u_i) + \frac{\partial}{\partial x_j}(\rho u_i u_j) = -\frac{\partial p}{\partial x_i} + \frac{\partial \tau_{ij}}{\partial x_j} + \frac{\partial}{\partial x_j}(-\rho \overline{u_i' u_j'}) \quad (12)$$

$$\frac{\partial}{\partial t}(\rho H) + \frac{\partial}{\partial x_i}(\rho u_i H) = \frac{\partial}{\partial x_i}\left[\left(\frac{\mu}{\sigma} + \frac{\mu_t}{\sigma_h}\right)\frac{\partial H}{\partial x_i}\right] + S_{rad} \quad (13)$$

In the equations above, H is the enthalpy, μ the viscosity, σ_h the turbulent Prandtl number, σ the Prandtl number and τ_{ij} the stress tensor. The term $(-\rho \overline{u_i' u_j'})$ represents the Reynolds stresses, modelled by the k-ε turbulence model. S_{rad} is a source term to include the radiation heat transfer, computed by the *P1* model.

The simulations carried out in the present work were performed using the open CFD software OpenFOAM. Using C++, an own OpenFOAM solver was programmed. Pressure-velocity coupling was achieved using the PISO (Pressure Implicit with Splitting of Operators) algorithm because it is recommended for transient calculations. A second order scheme was chosen to discretize the continuity, momentum, energy, and mass fraction equations. The time derivatives were discretized through a first order fully implicit scheme with a constant time step of 0.0005 s. Extensive convergence checks were taken in order to confirm that the computed results are independent of the time step and grid size. Concerning the turbulence model, the standard k-ε was selected for its robustness, economy and reasonable accuracy for a wide range of turbulent flows.

2.3 EXPERIMENTAL VALIDATION

The reliability of the CFD model to predict NO_x reduction was checked by comparison with experimental results developed by Ostberg *et al.* [28]. These authors employed flue gas from a natural gas burner with a water-cooled probe to adjust the temperature. This gas was injected in a tubular reactor 5000 mm in length and 50 mm in diameter, shown in Figure 1. The flue gas composition during the experiments was 550 ppm_{vol} NO, 73.4%$_{vol}$ N_2, 15.1%$_{vol}$ H_2O, 8%$_{vol}$ CO_2, 3.4%$_{vol}$ O_2 and the flow 940 nl/min. 1 nl/min injection of ammonia in crossflow was applied 1250 mm downstream from the inlet.

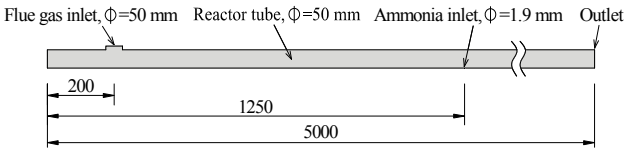

Figure 1. Experimental setup of Ostberg *et al.* [28].

The computational mesh employed to simulate the experiments of Ostberg *et al.* [28] is shown in Figure 2. It has 315,000 tetrahedral elements, refined in the zone close to the NH_3 inlet due to its small diameter. By virtue of the symmetry, only half of the domain was computed.

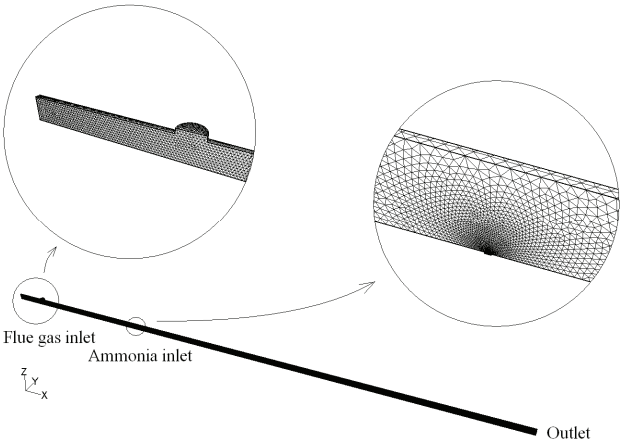

Figure 2. Computational mesh.

The results of NO relative change against temperature are indicated in Figure 3. This figure shows the experimental measurements and the numerical results using the models of Brouwer *et al.* [25] and Duo *et al.* [26], which provided errors of 9.6% and 16.3% respectively. As can be seen, both numerical models and the experimental measurements indicate the existence of a narrow temperature interval in which the NO reduction is efficient. If the temperature is too high, ammonia itself oxidizes to NO instead of reacting with NO. On the contrary, below the optimal temperature the reduction reactions are too slow and unreacted ammonia is emitted through the outlet. Despite some discrepancies, both numerical models are able to reproduce the main trends evidenced experimentally. The kinetic model of Duo *et al.* [26] is less accurate than that of Brouwer *et al.* [25],

specially at high temperatures. The reason is that Duo *et al.* [26] employed a limited number of experimental data, involving the concentrations 507 ppm_{vol} NO, 830 ppm_{vol} NH_3 and 4.1%$_{vol}$ O_2. For this reason, the model of Brouwer *et al.* [25] was employed in the simulation of the MAN 7S50MC marine engine, described in the following section.

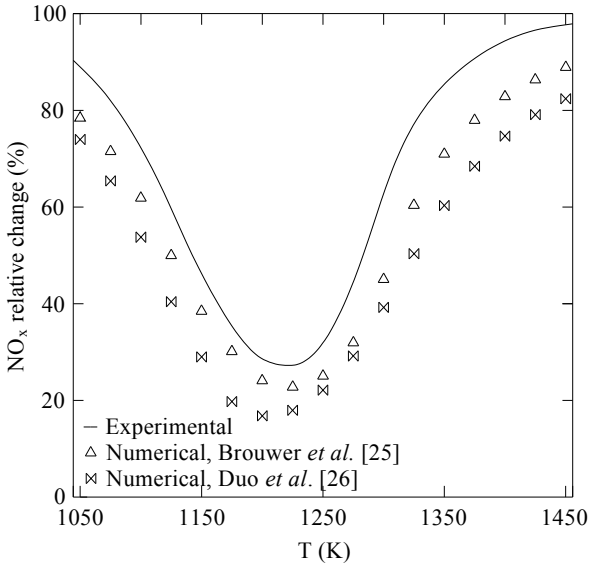

Figure 3. Comparison between numerical and experimental results.

3. CASE STUDIED

Once validated, the model of Browner *et al.* [25] was employed to simulate NO_x reduction in the MAN 7S50MC. This is a two-stroke, low speed, marine diesel engine with 7 cylinders, 50 cm bore, 191 cm stroke, 375028 cm^3 cylinder displacement volume and 127 rpm speed. Each cylinder has 16 intake ports on the cylinder liner close to the bottom dead center and one exhaust valve in the cylinder head. Figure 4 shows a photograph of the engine analyzed in the present work.

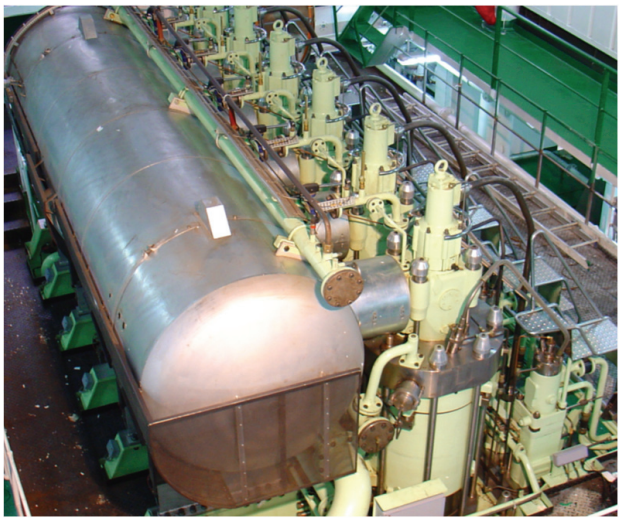

Figure 4. Engine studied in the present work.

Figure 5 shows the cylinder head. As can be seen, a direct injection is produced by two fuel injectors located near the outer edge of the combustion chamber. The direction of the injections is indicated in the plan view of Figure 6. More details about this engine can be consulted in previous works [11, 29].

The combustion process of this engine was numerically simulated and validated with experimental results elsewhere [11]. This previous work employed the open CFD software OpenFOAM and obtained the following pollutant emissions: 118 ppm_{vol} of CO, 472 ppm_{vol} of HC and 887 ppm_{vol} of NO_x. In the present work, NO_x reduction by ammonia injection, *i.e.*, Eqs. (5-10) were added to this previous model to simulate the combustion process with ammonia injection. To this end, ammonia was injected by two injectors. These were located next to the fuel injectors in order to facilitate the fuel-ammonia mixing. Figure 7 shows the grid at the start of the simulation, 20º before TDC (top dead center), and at TDC. As all cylinders are identical, only one of them was simulated. Only the combustion chamber (see Figure 1) was simulated. The inlet ports and exhaust valve remain closed during the entire simulation. The CFD simulation was carried out from 20º before TDC to the exhaust valve opening, 120º after TDC.

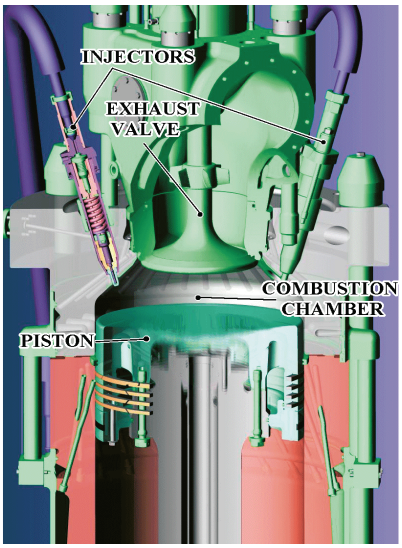

Figure 5. Cylinder head. Adapted from MAN B&W [30].

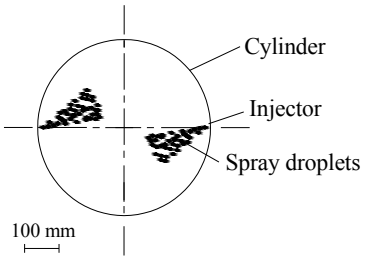

Figure 6. Direction of the fuel injections.

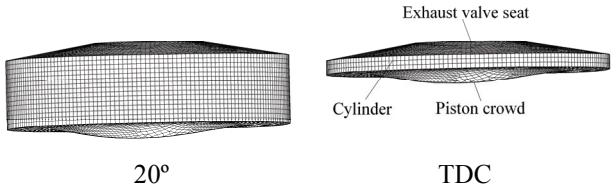

Figure 7. Computational mesh at 20 and TDC crankshaft angles.

4. RESULTS

As indicated in Figure 3, NO_x reduction is very sensible to temperature. For this reason, it is very important to select the appropriate instant of start of ammonia injection. Figure 8 indicates the NO_x relative change values against the start of ammonia injection. An injection temperature of 1200K and an ammonia to fuel ratio of 2% were employed. As can be seen, if the injection occurs too soon there is a deficient NO_x reduction because the temperature around the injectors is too high. On the contrary, late injections also promote a deficient NO_x reduction due to the low temperature around the injectors. The optimum NO_x reduction is obtained at 69.8º crankshaft angle at start of injection.

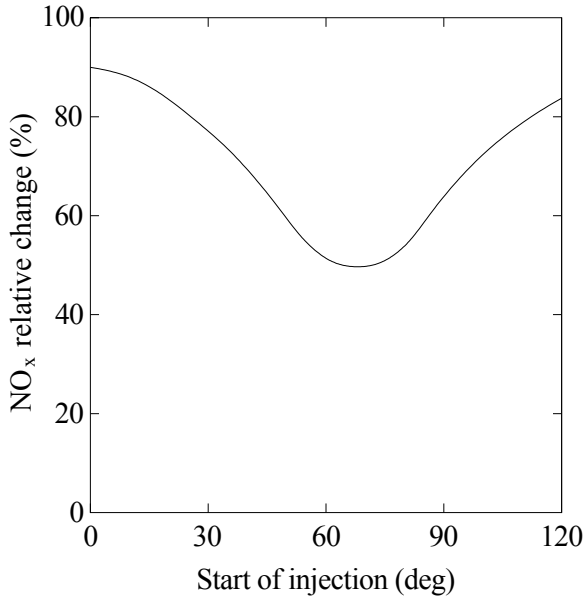

Figure 8. NO_x reduction against start of ammonia injection. Injection temperature = 1200K, ammonia to fuel ratio = 2%.

The temperature at which ammonia is injected is also very important. Figure 9 shows the NO_x relative change against this parameter. A start of injection of 69.8º and an ammonia to fuel ratio of 2% were employed. As in the previous case, low and high temperatures promote a deficient NO_x reduction. The optimal value is 1243 K.

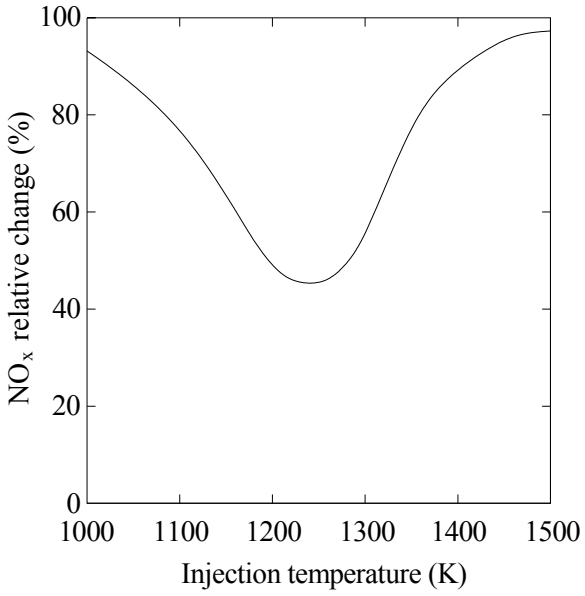

Figure 9. NO_x reduction against the injection temperature. Start of injection = 69.8º crankshaft angle, ammonia to fuel ratio = 2%.

In order to quantify the ammonia reduction capabilities, Figure 10 indicates the NO_x relative change against the ammonia to fuel ratio using the optimum values of temperature and start of injection, *i.e.*, 1243 K and 69.8º respectively. Besides, CO and HC emissions were included. These results were compared with the water addition procedure obtained in the previous paper [11], against the water to fuel ratio, given by Eq. (14). In this case, water was simulated as a water-fuel emulsion instead a pure water injection, thus employing the same temperature and start of injection of the fuel, 408K and -2º respectively. It is important to mention that practical applications do not reach 100% water to fuel ratios. This value was analyzed simply to indicate the capability of water addition to reduce NO_x emissions. Unfortunately, the results indicated in Figure 10 were not validated experimentally. Nevertheless, it was verified that the influence of water addition agrees with other experimental data obtained elsewhere [31].

$$\text{Water to fuel ratio (\%)} = \frac{\text{mass of water}}{\text{mass of fuel}} 100 \qquad (14)$$

As can be seen in Figure 10, NO_x reduction using ammonia drastically increases with increasing the ammonia to fuel ratio and reaches nearly 60% (41.6% relative change) at a 3.1% ratio. Beyond this, NO_x tends to increase slightly due to ammonia oxidation. Concerning NO_x reduction using water, an asymptotic tendency is obtained. Besides, the amount of water needed is much higher than that of ammonia.

Another conclusion obtained from Figure 10 is that water addition has a much more important effect on CO and HC

emissions. On the contrary, ammonia injection has a negligible effect on these pollutants. The reason is that the principle of actuation of water is very different to that of ammonia. The purpose of water addition is to lower the combustion temperature and thus reduce NO_x emissions. Figure 11 shows the temperature field at TDC, without water addition and with a 50% water to fuel ratio. The maximum temperature is lowered 78 K using 50% water addition. This temperature reduction is caused by the increase in the specific heat capacity of the cylinder gases (water has higher specific heat capacity than air) and reduced oxygen concentration. Due to the lower temperatures, water addition promotes an incomplete combustion and thus increments of CO and HC emissions. On the other hand, the purpose of ammonia injection is to react with NO_x without reduce the combustion temperature. For this reason, the influence on CO and HC emissions is negligible.

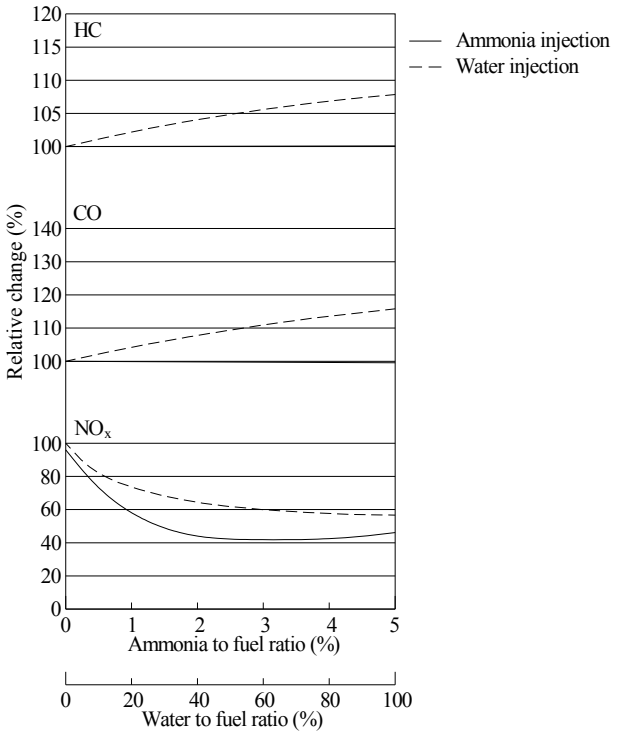

Figure 10. Relative change in pollutants using ammonia (start of injection = 69.8º crankshaft angle, injection temperature = 1243K) and water (start of injection = -2º crankshaft angle, injection temperature = 408K).

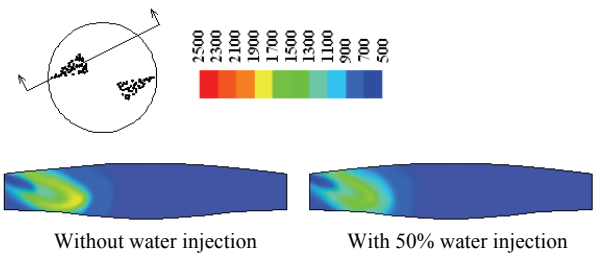

Figure 11. Temperature field (K) at TDC, without water injection and with 50% water injection.

5. CONCLUSIONS

The present paper proposed a CFD model to simulate NO_x reduction by ammonia injection in the MAN 7S50MC marine engine. The strongest motivation was given by the current legislation, for which the most important pollutant from marine diesel engines that must be reduced is NO_x.

Results obtained using ammonia were compared to those using water addition. It was verified that ammonia can reduce a higher amount of NO_x with a negligible effect on both HC and CO emissions. Water addition is less efficient to reduce NO_x and besides increase HC and CO emissions due to an incomplete combustion. Nevertheless, the main disadvantage of ammonia injection is that it needs a very accurate control system due to the strong dependence on the injection temperature, injection instant and ammonia to fuel ratio. Another disadvantage of this procedure is that ammonia is toxic and an accidental ammonia leak from the tank could cause deaths. There are other NO_x reducing agents such as urea, cyanuric acid, etc, but these are too expensive.

6. ACKNOWLEDGEMENTS

The authors would like to express their gratitude to "Talleres Pineiro, S.L.", sale and repair of marine engines.

7. REFERENCES

1. LENG, X. Y.; LONG, W. Q.; FENG, L. Y.; DONG, Q.; LI, H. Y.; WANG, X. J.; YU, X. J.; WANG, A. G. Numerical simulation research into effects of injection rates on performance and emissions of diesel engine, *Journal of Dalian University of Technology, volume 51(2), pp. 180–187*, 2011.
2. ANDREADIS, P.; ZOMPANAKIS, A.; CHRYSSAKIS, C.; KAIKTSIS, L. Effects of the fuel injection parameters on the performance and emissions formation in a large-bore marine diesel engine, *International Journal of Engine Research, volume 12(1), pp. 14–29*, 2011.
3. MORENO GUTIERREZ, J; RODRIGUEZ MAESTRE, I.; SHAFIK, T.; DURAN GRADOS, C.V.; CUBILLAS, P.R., The influence of injection timing over nitrogen oxides formation in marine diesel engines, *Journal of Marine Environmental Engineering, volume. 16, pp. 1-10,* 2006.
4. AL-SENED, A.; KARIMI, E., Strategies for NO_x reduction in heavy duty engines, *23rd CIMAC Congress*, 2001.
5. FANKHAUSER, S.; HEIM, K., The Sulzer RT-flex Launching the era of common rail on low

speed engines, *23rd CIMAC Congress*, 2001.

6. PANAGIOTIS, A.; CHRYSSAKIS, C.; KAIKTSIS, L., Optimization of injection characteristics in a large marine diesel engine using evolutionary algorithms. *SAE Paper 2009-01-1448*, 2009.
7. BLUDSZUWEIT, S.; PITTERMAN, R.; STANEV, A., Investigations into emission characteristics of large two stroke cross head engines running on heavy fuel, *CIMAC 1998, volume 4, pp 829,* 1998.
8. HOLTBECKER, R.; GEIST, M. Emissions Technology. Sulzer RTA Series, Exhaust Emissions Reduction Technology for Sulzer Marine Diesel Engines, *Wärtsilä NSD,* 1998.
9. BIGOS, P.; PUSKAR, M. Influence of cylinder shape and combustion space on engine output characteristic of two-stroke combustion engine. *Zdvihací zařízení v teorii a praxi, volume 3,* 2008.
10. LARBI, N.; BESSROUR, J. Measurement and simulation of pollutant emissions from marine diesel combustion engine and their reduction by water injection. *Advances in Engineering Software, volume 41(6), pp. 898-906*, 2010.
11. LAMAS, M.I.; RODRIGUEZ, C.G.; AAS, H.P., Computational fluid dynamics analysis of NOx and other pollutants in the MAN B&W 7S50MC marine engine and effect of EGR and water addition, *Transactions RINA, Vol 155, Part A2, Internacional Journal of Maritime Engineering, April-June 2013, pp. A81-A88,* 2013.
12. MILLO, F.; BERNARDI, M.G.; DELNERI, D., Computational analysis of internal and external EGR strategies combined with Miller cycle concept for a two stage turbocharged medium speed marine diesel engine, *SAE Paper 2011-01-1142,* 2011.
13. LARBI, N.; BESSROUR, J. Measurement and simulation of pollutant emissions from marine diesel combustion engine and their reduction by exhaust gas recirculation. *Journal of Mechanical Science and Technology, volume 22, pp. 2263-2273*, 2008.
14. HOLTBECKER, R.; GEIST, M. Emissions Technology, *Wärtsilä NSD, Finland,* 1998.
15. LAMAS, M.I.; RODRÍGUEZ, C.G. Emissions from marine engines and NOx reduction methods, *Journal of Maritime Research, volume 9(1), pp.77-82,* 2012.
16. JAYARAN, V.; NIGAM, A.; WELCH, W.A.; MILLAR, J.W.; COCKER, I.I., Effectiveness of emission control technologies for auxiliary engines on ocean-going vessels, *Journal of the Air & Waste Management Association, volume 61(1), pp 14-21,* 2011.
17. LARBI, N.; BESSROUR, J. Measurement and simulation of pollutant emissions from marine diesel combustion engine and their reduction by ammonia injection, *Advances in Mechanical Engineering. 459813*, 2009.
18. MIYAMOTO, N.; OGAWA, H.; WANG, J.; SHUDO, T.; YAMAZAKI, K. Diesel NO_x reduction with ammonium deoxidizing agents directly injected into the cylinder, *International Journal of Vehicle Design, volume 16(1), pp. 71-79,* 1995.
19. NAM, C.; GIHONG, K; MOK, Y. Diesel engine NO_x reduction by SNCR under simulated flow reactor conditions, *Environmental Engineering Research, volume 11(3), pp. 149-155,* 2006.
20. NAM, C.M.; GIBBS, B.M., Application of the Thermal DeNOx process to diesel engine $DeNO_x$: An experimental and kinetic modeling study, *Fuel, volume 81, pp. 1359-1367,* 2002.
21. LYON, R.K. Method for the reduction of the concentration of NO in combustion effluents using ammonia. *U.S. Patent, no. 3, 900, 554,* 1975.
22. MILLER, J.A.; BROWMAN, C.T. Mechanism and modelling of nitrogen chemistry in combustion, *Progress in Energy and Combustion Science, volume 15, pp. 287-338,* 1989.
23. GLARBORG, P.; DAM-JOHANSEN, K.; MILLER, J.A.; KEE, R.J.; COLTRIN, M.E. Modeling the thermal $DeNO_x$ process in flow reactors. Surface effects and nitrous oxide formation, *International Journal of Chemical Kinetics, volume 26, pp. 421-436,* 1994.
24. MILLER, J.A.; Glarborg, P. Modeling the formation of N_2O and NO_2 in the thermal $DeNO_x$ process, *Springer Series in Chemical Physics, volume 61, pp. 318-333,*1996.
25. BROUWER, J.; HEAP, M.P.; PERSHING, D.W.; SMITH, P.J. A model for prediction of selective noncatalytic reduction of nitrogen oxides by ammonia, urea, and cyanuric acid with mixing limitations in the presence of CO, *26th Symposium (International) on Combustion, pp. 2117-2124,*1996.
26. DUO, W.; DAM-JOHANSEN, K.; OSTERGAARD, K. Kinetics of the gas-phase reaction between nitric oxide, ammonia and oxygen, *The Canadian Journal of Chemical Engineering, volume 70, pp. 1014-1020,*1992.
27. VERSTEEG, H.K.; MALALASEKERA, W. An introduction to computational fluid dynamics. The finite volume method, *2nd Edition, Pearson Prentice Hall*, 2007.
28. OSTBERG, M.; DAM-JOHANSEN, K.; JOHNSSON, J.E. Influence of missing on the SNCR process, *Chemical Engineering Science, volume 52, pp. 2511-1525,* 1997.
29. LAMAS, M.I.; RODRIGUEZ, C.G. CFD analysis of the scavenging process in the MAN B&W 7S50MC two-stroke diesel marine engine*, Journal of Ship Research, volume 56(3), pp. 154–161,* 2012.

30. MAN Diesel. MAN B&W S50MC Project Guide, 6th Ed., *MAN Diesel, Denmark,* 2009.
31. PAYRI F.; DESANTES, J.M., Motores de combustión interna alternativos. *1st Edition. Editorial Reverté, Spain,* 2011.

